THE JOURNAL OF BIOLOGICAL CHEMISTRY
Vol. 272, No. 11, Issue of March 14, pp. 6994–7002, 1997

Printed in U.S.A.

Comparative Kinetic Analysis and Substrate Specificity of the Tandem Catalytic Domains of the Receptor-like Protein-tyrosine Phosphatase α*

(Received for publication, November 11, 1996, and in revised form, January 14, 1997)

Li Wu‡, Arjan Buist§, Jeroen den Hertog§, and Zhong-Yin Zhang‡¶

From the ‡Department of Molecular Pharmacology, Albert Einstein College of Medicine, Bronx, New York 10461 and the §Hubrecht Laboratory, Netherlands Institute for Developmental Biology, Uppsalalaan 8, 3584 CT Utrecht, The Netherlands

The catalytic activity and substrate specificity of protein-tyrosine phosphatase α (PTPα) is primarily controlled by the membrane proximal catalytic domain (D1). The membrane distal (D2) domain of PTPα by itself is a genuine PTPase, possessing catalytic activity comparable to that of D1 using aryl phosphates as substrates. Surprisingly, k_{cat} and k_{cat}/K_m for the D2-catalyzed hydrolysis of phosphotyrosine-containing peptides are several orders of magnitude reduced in comparison with those of D1. Substitution of the putative general acid/base Glu-690 in D2 by an Asp, which is invariably found in the WPD motifs in all cytoplasmic PTPases and all the D1 domains of receptor-like PTPases, only increases the k_{cat} for D2 by 4-fold. Thus the much reduced D2 activity toward peptide substrates may be due to structural differences in the active sites other than the general acid/base. Alternatively, the D2 domain may have a functional active site with a highly stringent substrate specificity. PTPα display modest peptide substrate selectivity and are sensitive to charges adjacent to phosphotyrosine. In the sequence context of DADEpYLIPQQG (where pY stands for phosphotyrosine), the minimal sizes recognized by PTPα are either ADEpYLI or DADEpY-NH_2.

Protein-tyrosine phosphatases (PTPases)[1] catalyze the hydrolysis of phosphoryl groups on tyrosine residues in proteins that are introduced by protein-tyrosine kinases. A tightly balanced phosphatase and kinase activity is required for proper cellular functions (1, 2). PTPases constitute a growing family (>70 members) of enzymes that can be structurally categorized into two major groups: receptor-like (transmembrane) and nonreceptor (intracellular) PTPases (3). Although many PTPases are proteins of greater than 400 amino acids, their catalytic domains are usually contained within a span of 250 residues referred to as the PTPase domain. This domain is the only structural element that has amino acid sequence identity among all PTPases from bacteria to mammals (4). The hallmark that defines the PTPase family is the active site sequence (H/V)**C**$(X)_5$**R**(S/T), called the PTPase signature motif in the catalytic domain (5, 6). The receptor-like PTPases, exemplified by the leukocyte phosphatase CD45, generally have an extracellular domain, a single transmembrane region, and cytoplasmic PTPase domain(s). The intracellular PTPases, exemplified by PTP1B, contain a single catalytic domain and various amino- or carboxyl-terminal extensions including SH2 domains that may have targeting or regulatory functions.

The cytoplasmic segment of many receptor-like PTPases have two tandem PTPase domains: D1, which is proximal to the membrane, and D2, which is distal to the membrane. The existence of homologous PTPase domains in the receptor-like PTPases raises the interesting possibility of differential functions or regulations of the two domains. However, the significance of the repeated PTPase domain in the receptor-like PTPases is not clear. One important question is whether both PTPase domains in the receptor-like phosphatases are catalytically active? There is evidence that suggest that D2 is catalytically inactive and may only play, if any, a regulatory role. This is supported by the following observations. First, there are receptor-like PTPases that lack either the essential Cys residue within the PTPase signature motif in D2 (HPTPγ and RPTPβ) (7, 8) or the entire D2 domain (PTPβ and DPTP10D) (7, 9–11). Second, replacement of the Cys residue in the signature motif of D1 in LAR and CD45 abolishes the phosphatase activity while the same substitution in the signature motif in D2 has little or no effect on PTPase activity (12, 13). Third, recombinant D1 of LAR or LCA (13–15) exhibits phosphatase activity that are identical to the wild-type double domain PTPase, whereas constructs for D2 alone show no measurable activity (13, 14). Last, inactivation of D1 in PTPα (16) or CD45 (17) results in loss of biological activity of these two PTPases, indicating that catalytic activity of D1 is essential for the function of these PTPases.

On the other hand, there are reports that indicate that in some receptor-like PTPases the second domain may display catalytic activity. For example, elimination of the critical Cys in D1 of LAR or PTPμ results in >99% loss of activity (18, 19). The residual activity (usually less than 0.1%) is concluded to be associated with D2. Recent evidence suggest that under some conditions D2 of CD45 could be a viable phosphatase (20), and that certain structural elements in D2 may be required for full expression of CD45 PTPase activity in D1 (21, 22). The most compelling data that identify intrinsic phosphatase activity with D2 come from work on PTPα. Working with purified recombinant individual PTPase domains, Wang and Pallen (23) showed that D2 of PTPα could hydrolyze *p*-nitrophenyl phosphate and dephosphorylate a phosphotyrosine-containing synthetic peptide, albeit at a very low rate relative to D1. Furthermore, recombinant RPTPα containing an inactive D1

* This work was supported by National Institutes of Health Grant CA69202 (to Z.-Y. Z), a grant from the Life Sciences Foundation/Netherlands Organization for Scientific Research (SLW/NWO) (to A. B.), and a grant from the Dutch Cancer Society (to J. d. H.). The costs of publication of this article were defrayed in part by the payment of page charges. This article must therefore be hereby marked "*advertisement*" in accordance with 18 U.S.C. Section 1734 solely to indicate this fact.

¶ To whom correspondence should be addressed: Dept. of Molecular Pharmacology, Albert Einstein College of Medicine, 1300 Morris Park Ave., Bronx, NY 10461. Tel.: 718-430-4288; Fax: 718-430-8922.

[1] The abbreviations used are: PTPase, protein-tyrosine phosphatase; *p*NPP, *p*-nitrophenyl phosphate; EGF, epidermal growth factor.

still retained a low but measurable activity against the Tyr-789-phosphorylated catalytically inactive RPTPα (24).

PTPα is a receptor-like PTPase that has a small, highly glycosylated extracellular segment, a transmembrane region, and an intracellular segment possessing two PTPase domains (7, 25). PTPα is expressed ubiquitously, although the levels of expression vary. During mouse development, enhanced expression was detected in derivatives of the neural crest (26). Evidence suggest that it may be involved in the activation of c-*src* by dephosphorylation of Tyr-527 (16, 27) and the down-regulation of insulin receptor signaling (28). To better understand the relative importance of the two PTPase domain in PTPα catalysis, we have compared their intrinsic phosphatase activities using a variety of low molecular weight aryl phosphates and Tyr(P)-containing peptides.

EXPERIMENTAL PROCEDURES

Materials—*p*-Nitrophenyl phosphate (*p*NPP), β-naphthyl phosphate, *O*-phospho-L-tyrosine, and 4-methylumbelliferyl phosphate were purchased from Sigma. 4-Acetylphenyl phosphate, 4-ethoxycarbonylphenyl phosphate, 3-chlorophenyl phosphate, and 4-methylphenyl phosphate were synthesized and characterized as described earlier (29). Glutathione-agarose beads and human thrombin were purchased from Sigma. Phosphotyrosine-containing peptides were synthesized, purified, and characterized as described previously (30). Peptides DTSSVLpYTAVQ ($PDGFR^{1003–1013}$), EGDNDpYIIPL[2] ($PDGFR^{1016–1025}$), and Ac-DAFSDpYANFK ($PTP\alpha^{784–793}$) were prepared by the Laboratory of Macromolecular Analysis of Albert Einstein College of Medicine. Vanadium (V) oxide (99.99%) was obtained from Aldrich. Solutions were prepared using deionized and distilled water.

Constructs and Mutagenesis—Expression vectors for bacterial expression of RPTPα glutathione *S*-transferase fusion proteins were derived by insertion of polymerase chain reaction-generated *Nco*I-*Hin*dIII fragments into pGEX-KG opened with *Nco*I and *Hin*dIII (31). The bacterial expression vector encoding the complete cytoplasmic region of RPTPα (residues 167–793; numbering according to Sap *et al.* (25)), bPTPα,[3] has been described (24). The expression vectors for bPTPα-D1 (residues 167–503) and bPTPα-D2 (residues 504–793) were derived using the oligonucleotide pairs NI, CII and NIV, CI, respectively: NI, 5′-GCGCCATGGCGAAGAAATACAAGCAA, CII, 5′-CCCTCAAGCTTCCAGTTCTGTGTCCCCATA, NIV, 5′-CCCATGGCTTCTCTAGAAACC, CI, 5′-CGCAAGCTTTCACTTGAAGTTGGC. Site-directed mutagenesis was done on the full-length RPTPα cDNA in pBluscript SK−. Mutations were verified by sequencing and subsequently the corresponding glutathione *S*-transferase fusion protein expression vectors were constructed as described above. The oligonucleotides that were used for site-directed mutagenesis are: RPTPα-D401A, 5′-AGCTGGCCAGCCTTTGGGGTG, and RPTPα-E690D, 5′-GGCTGGCCTGATGTGGGCATC.

Recombinant Enzymes—The PTPα-glutathione *S*-transferase fusion protein constructs were transformed into *Escherichia coli* BL21(DE3). A 10-ml overnight culture of BL21(DE3) cells containing pGEX recombinant plasmids for PTPα were diluted 100-fold into 1 liter of 2×YT medium with 100 μg/ml ampicillin. The culture was grown at 37 °C until the absorbance at 600 nm reached 0.6. Expression of glutathione *S*-transferase fusion proteins were then induced by the addition of 100 μM isopropyl-1-thio-β-D-galactopyranoside. Following the induction, the cells were allowed to grow overnight at room temperature. Purification of the PTPα-glutathione *S*-transferase fusion proteins by glutathione-agarose beads and the subsequent thrombin cleavage of the glutathione *S*-transferase fusion protein were accomplished as described (31). The recombinant PTPα proteins were at least 90% in purity as judged by SDS electrophoresis.

pH and Leaving Group Dependences—The PTPase activity was assayed at 30 °C in a reaction mixture (0.2 ml) containing appropriate concentrations of *p*NPP as substrate. Buffers used were as follow: pH 4.0–5.5, 100 mM acetate; pH 5.5–6.5, 50 mM succinate; pH 6.6–7.3, 50 mM 3,3-dimethylglutarate, and pH 7.5–9.0, 50 mM Tris. All of the buffer systems contained 1 mM EDTA and the ionic strength of the solutions were kept at 0.15 M using NaCl. The reaction was initiated by addition of enzyme and quenched after 2–3 min by addition of 1 ml of 1 N NaOH. The nonenzymatic hydrolysis of the substrate was corrected by measuring the control without the addition of enzyme. The amount of product *p*-nitrophenol was determined from the absorbance at 405 nm using a molar extinction coefficient of 18,000 M^{-1} cm^{-1}. Michaelis-Menten kinetic parameters were determined from a direct fit of the *v versus* [S] data to the Michaelis-Menten equation (Equation 1) using the nonlinear regression program GraFit (Erithacus Software).

$$v = \frac{k_{cat}[E][S]}{K_m + [S]} \quad \text{(Eq. 1)}$$

pH dependence of k_{cat} data were fitted to Equation 2 using a nonlinear least-squares regression program (KaleidaGraph, Synergy Software). In Equation 2, k_{cat}^{lim}, the pH independent turnover number, and K_1^{app} and K_2^{app}, are the apparent ionization constants of the enzyme-substrate complex (32). Leaving group dependence was conducted at pH 6.0 and 30 °C with aryl phosphates having leaving group pK_a values from 7.14 to 10.26 (33).

$$k_{cat} = \frac{k_{cat}^{lim}}{1 + \frac{H}{K_1^{app}} + \frac{K_2^{app}}{H}} \quad \text{(Eq. 2)}$$

Determination of Kinetic Constants Using Tyr(P)-containing Peptides as Substrates—Initial rates for the PTPase catalyzed hydrolysis of Tyr(P)-containing peptide substrates were determined by following the production of inorganic phosphate (30). k_{cat} and K_m values were calculated from a direct fit of the *v versus* [S] data to Equation 1 using the nonlinear regression program GraFit (Erithacus Software). The PTPase-catalyzed hydrolysis of Ty(P)-containing peptides can also be monitored continuously at 305 nm for the increase in tyrosine fluorescence with excitation at 280 nm (30). When $[S] \ll K_m$, Equation 1 reduces to Equation 3,

$$v = \frac{k_{cat}}{K_m}[E][S] \quad \text{(Eq. 3)}$$

Under this condition, the reaction is first-order with respect to [S]. At a given enzyme concentration, the observed apparent first-order rate constant is equal to $(k_{cat}/K_m)[E]$. The substrate specificity constant k_{cat}/K_m value is calculated by dividing the apparent first-order rate constant by the enzyme concentration. Fluorometric determinations were performed on a Perkin-Elmer LS50B fluorometer. The instrument was equipped with a water-jacketed cell holder, permitting maintenance of the reaction mixture at the desired temperature (30 °C).

Inhibition Studies—The following procedure for the preparation of stock solution of sodium orthovanadate was adopted from Dr. Mike Gresser's laboratory: vanadium (V) oxide was dissolved in 1 mol eq per vanadium atom of 1.0 M aqueous NaOH. The resulting orange solution (mainly decavanadate) was boiled, allowed to stand overnight, and pH adjusted to 10. The final solution was colorless containing mainly orthovanadate (34). The inhibition constants for inorganic phosphate, arsenate, vanadate, and *p*-nitrophenol were determined for the phosphatases in the following manner. When oxyanions were used as inhibitors, the initial rate at various *p*NPP concentrations was measured by following the production of *p*-nitrophenol (35). When *p*-nitrophenol was used as an inhibitor, the initial rate at various *p*NPP concentrations was measured by following the production of inorganic phosphate (33). The inhibition constant and inhibition pattern were evaluated using a direct curve-fitting program KINETASYST (IntelliKinetics, State College, PA).

RESULTS

Kinetic Parameters of Various Forms of RPTPα Using pNPP and Tyr(P)-containing Peptides as Substrates—To study the catalytic properties of the individual PTPase domains of RPTPα, we have generated glutathione *S*-transferase fusion protein constructs that encode the cytoplasmic portions of RPTPα,[4] bPTPα[3] (amino acid residues 167–793), bPTPα-D1 (amino acid residues 167–503), and bPTPα-D2 (amino acid

[2] Where pY stands for phosphotyrosine.

[3] "b" in bPTPα stands for bacterial to distinguish between the full-length RPTPα and the bacterially expressed recombinant RPTPα.

[4] Since the human protein-tyrosine phosphatase α is called PTPα, we have designated the mouse homolog RPTPα to avoid confusion. Mouse and human PTPα are almost identical in their cytoplasmic regions. There are only four residues that are different between mouse and human, and all four are conservative changes.

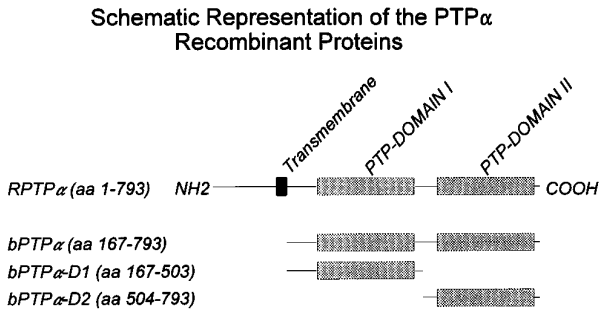

FIG. 1. **Schematic representation of the PTPα recombinant proteins that were used in this study.** For comparison, full-length RPTPα is depicted as well. *Solid box*, transmembrane domain; *hatched boxes*, PTPase domains. Numbering of the amino acid residues refers to the RPTPα coding sequence according to Ref. 25.

residues 504–793). A schematic representation of RPTPα, bPTPα, bPTPα-D1, and bPTPα-D2 is shown in Fig. 1. Glutathione *S*-transferase fusion proteins were expressed in *E. coli* BL21(DE3) and affinity purified on glutathione-agarose beads. Recombinant bPTPα, bPTPα-D1, and bPTPα-D2 were cleaved from the agarose bead-bound glutathione *S*-transferase with thrombin (31). The purity of bPTPα, bPTPα-D1, and bPTPα-D2 were general greater than 90% as judged by SDS-polyacrylamide gel electrophoresis (data not shown). Table I summarizes the steady-state kinetic parameters of the various forms of RPTPα using *p*NPP as a substrate. Thus, bPTPα (which contains both D1 and D2) exhibits kinetic parameters that are similar to those of bPTPα-D1. Interestingly, the k_{cat} value for D2 is only 10-fold lower than that of D1 while the K_m is 5-fold higher.

We next compared the ability of the individual PTPase domains to dephosphorylate Tyr(P)-containing peptides corresponding to Tyr autophosphorylation sites in platelet-derived growth factor receptor and EGF receptor, or the Tyr phosphorylation site (Tyr-789) in the COOH-terminal of RPTPα (24). The dephosphorylation reaction was followed by monitoring the production of inorganic phosphate with a colorimetric procedure (30). Kinetic constants for the hydrolysis of peptide substrates are listed in Table II. In comparison with the double PTPase domain-containing bPTPα, bPTPα-D1 displays slightly reduced k_{cat} values toward the peptide substrates, but the K_m values are indistinguishable. However, in contrast to small nonpeptidic substrate *p*NPP, the k_{cat} values for the bPTPα-D2-catalyzed hydrolysis of Tyr(P)-containing peptides decrease by 2 to 3 orders of magnitude compared with bPTPα-D1, while the K_m values increase by 1 to 2 orders of magnitude. Thus, the combined effects translate into a difference in substrate specificity constant (k_{cat}/K_m) in the range of 8,000 to 40,000-fold in favor of bPTPα-D1 over bPTPα-D2.

The Conserved General Acid/Base in the PTPase Domains—To begin to gain insight into the structural basis for the differential activity exhibited by D1 and D2, we have performed an amino acid sequence alignment for both of the PTPase domains in several receptor-like PTPases including RPTPα (Fig. 2). Invariant residues in D1 and D2 are listed below the sequence alignment. It is clear that D1 is more conserved than D2. Previous biochemical studies have demonstrated that the Cys residue in the PTPase signature motif (H/V)**C**$(X)_5$**R**(S/T) is essential for phosphatase activity and formation of a covalent cysteinyl phosphoenzyme intermediate (39–41). Mutations at the Cys residue result in complete loss of phosphatase activity. The invariant Arg residue in the signature motif has been shown to play an important role in substrate binding and transition state stabilization (5). Substitutions of Arg-409 in the *Yersinia* PTPase by either a Lys or an Ala cause a decrease in k_{cat} by nearly 4 orders of magnitude. In addition to nucleophilic catalysis and transition state stabilization, PTPases also utilize an invariant Asp residue in the WPD motif (Fig. 2) to facilitate the catalytic turnover: the Asp residue acts as a general acid to donate a proton to the phenolate leaving group in the phosphoenzyme formation step, while it acts as a general base to activate a nucleophilic water molecule in the phosphoenzyme hydrolysis step (4, 42). Replacement of Asp-356 by an Asn in *Yersinia* PTPase reduces the turnover number by 3 orders of magnitude. As can be seen in Fig. 2, the PTPase signature motif and the WPD motif are strictly conserved among the D1 domains. These two motifs are not conserved among the D2 domains.

TABLE I
Steady-state kinetic constants for various forms of RPTPα using pNPP as a substrate

All measurements were made at pH 6 and 30 °C.

	k_{cat}	K_m
	s^{-1}	mM
bPTPα	9.9 ± 0.3	3.6 ± 0.2
bPTPα-D1	9.1 ± 0.2	3.5 ± 0.2
bPTPα-D1/D401A	0.010 ± 0.0005	3.7 ± 0.4
bPTPα-D2	0.96 ± 0.03	18 ± 1
bPTPα-D2/E690D	4.1 ± 0.1	24 ± 4

A closer examination of the sequence alignment shows that in the D2 domain of PTPγ, the essential Cys and Arg residues in the active site are replaced by an Asp and a Ser, respectively. Furthermore, the Asp residue in the WPD motif is replaced by an Asn. Thus, it is unlikely that the second PTPase domain of PTPγ will possess any catalytic activity. Although the active site Cys is retained in the D2 domain of CD45, it lacks the critical Arg residue while the Asp residue is substituted by a Val. It is thus questionable whether the second PTPase domain of CD45 will exhibit any significant phosphatase activity.[5] Interestingly, the D2 domains of PTPα, PTPε, and LAR preserve all of the essential features of the PTPase signature motif, but the Asp residue in the WPD motif has been switched to a Glu. Based on the sequence alignment, Asp-401 is the putative general acid/base in the WPD motif in bPTPα-D1 whereas Glu-690 is the putative general acid/base in the WPE motif in bPTPα-D2. It is found that replacement of Asp with Glu or vice versa generally leads to a reduction of up to 3 orders of magnitude in catalytic efficiency in enzymes that require a carboxylate group as a general acid/base (43–46). Since an Asp is always found to be the general acid/base in the catalytic domains of cytoplasmic PTPases and the D1 domains of receptor-like PTPases, and since the D2 domains of receptor-like PTPases have much reduced catalytic activity, we asked the following question: can substitution of Glu-690 by an Asp in bPTPα-D2 increase its catalytic activity to a level comparable to bPTPα-D1?

To answer this question, we have converted Glu-690 in bPTPα-D2 to an Asp by site-directed mutagenesis. We have also made the Asp-401 to Ala mutation in bPTPα-D1 to test the importance of the Asp residue in the WPD motif. Although

[5] A previous study suggested that the D2 domain of CD45 was a functional PTPase (20). This was based on the following observations: 1) phosphatase activity could be detected when CD45 lacking the PTPase signature region in D1 was expressed in mammalian cells, and 2) a proteolytically cleaved fragment of CD45 containing most of D2 and the COOH-terminal part of D1 (including the PTPase signature sequence) displayed phosphatase activity. Although it is possible that the D2 domain of CD45 may employ a different mechanism from the one used by all the cytoplasmic PTPases and the D1 domains of receptor PTPases for phosphate monoester hydrolysis (see above), this needs to be further evaluated and verified.

TABLE II

Summary of kinetic constants with Tyr(P)-containing peptides as substrates

All measurements were made at pH 6 and 30 °C.

Substrate/enzyme	k_{cat}	K_m	k_{cat}/K_m
	s^{-1}	mM	$M^{-1}\ s^{-1}$
DTSSVLpYTAVQ (PDGFR$^{1003–1013}$)			
bPTPα	34 ± 1	0.18 ± 0.02	(1.9 ± 0.2) × 10^5
bPTPα-D1	26 ± 1	0.15 ± 0.02	(1.7 ± 0.2) × 10^5
bPTPα-D2	0.011 ± 0.001	1.5 ± 0.3	7.3 ± 2
bPTPα-D2/E690D	0.038 ± 0.002	1.4 ± 0.3	27 ± 6
EGDNDpYIIPL (PDGFR$^{1016–1025}$)			
bPTPα	21 ± 0.6	0.37 ± 0.02	(0.57 ± 0.06) × 10^5
bPTPα-D1	14 ± 0.3	0.32 ± 0.01	(0.44 ± 0.04) × 10^5
bPTPα-D2	0.0074 ± 0.0005	3.0 ± 0.3	2.5 ± 0.3
bPTPα-D2/E690D	0.032 ± 0.016	3.2 ± 1.7	10 ± 7
Ac-DAFSDpYANFK (PTPα$^{784–793}$)			
bPTPα	13 ± 1	0.27 ± 0.05	(0.48 ± 0.1) × 10^5
bPTPα-D1	9.7 ± 0.6	0.29 ± 0.04	(0.33 ± 0.05) × 10^5
bPTPα-D2	0.025 ± 0.003	5.9 ± 0.9	4.2 ± 0.8
bPTPα-D2/E690D	0.066 ± 0.006	5.5 ± 0.7	12 ± 2
DADEpYLIPQQG (EGFR$^{988–998}$)			
bPTPα-D1	9.1 ± 0.3	0.060 ± 0.006	(1.5 ± 0.2) × 10^5
bPTPα-D2	0.017 ± 0.020	4.5 ± 3.2	3.8 ± 4.2
TAENAEpYLRV (EGFR$^{1167–1176}$)			
bPTPα-D1	6.1 ± 0.3	0.22 ± 0.04	(0.28 ± 0.05) × 10^5
bPTPα-D2	0.0061 ± 0.0007	1.7 ± 0.10	3.6 ± 0.4

```
mPTPα-D1   (256)   NKEKNRYVNILPYDHSRVHL--------TPVEGVPDSDYINASFINGYQEKNKFIAAQGPKEETVNDFWRMIWEQNTATIVMVTNLKERK
hPTPε-D1   (140)   NREKNRYPNILPNDHSRVIL--------SQLDGIPCSDYINASYIDGYKEKNKFIAAQGPKQETVNDFWRMVWEQKSATIVMLTNLKERK
hCD45-D1   (675)   NQNKNRYVDILPYDYNRVEL--------SEINGDAGSNYINASYIDGFKEPRKYIAAQGPRDETVDDFWRMIWEQKATVIVMVTRCEEGN
hLAR-D1   (1365)   NKPKNRYANVIAYDHSRVIL--------TSIDGVPGSDYINANYIDGYRKQNAYIATQGPLPETMGDFWRMVWEQRTATVVMMTRLEEKS
hPTPγ-D1   (874)   NKHKNRYINILAYDHSRVKL------RPLPGKDSKHSDYINANYVDGYNKAKAYIATQGPLKSTFEDFWRMIWEQNTGIIVMITNLVEKG

mPTPα-D2   (549)   NMKKNRVLQIIPYEFNRVII--------PVKRGEENTDYVNASFIDGYRQKDSYIASQGPLLHTIEDFWRMIWEWKSCSIVMLTELEERG
hPTPε-D2   (432)   NMKKARVIQIIPYDFNRVIL--------SMKRGQEYTDYINASFIDGYRQKDYFIATQGPLAHTVEDFWRMIWEWKSHTIVMLTEVQERE
hCD45-D2   (977)   PYDYNRVPLKHELEMSKESEHDSDESSDDDSDSEEPSKYINASFIMSYWKPEVMIAAQGPLKETIGDFWQMIFQRKVKVIVMLTELKHGD
hLAR-D2   (1654)   NKFKNRLVNIMPYELTRVCL--------QPIRGVEGSDYINASFLDGYRQQKAYIATQGPLAESTEDFWRMLWEHNSTIIVMLTKLREMG
hPTPγ-D2  (1175)   NKEKNRNSSVVPSERARVGL--------APLPGMKGTDYINASYIMGYYRSNEFIITQHPLPHTTKDFWRMIWDHNAQIIVMLPDNQSL-

Conserved-D1       N--KNRY------D--RV-L------------------YINA----G--------IA-QGP---T--DFWRM-WEQ-----VM-T---E--
Conserved-D2       -----R-----------------------------------YINAS----Y------I--Q-PL-----DFW-M--------IVML-------

                                                                                                    *
mPTPα-D1   (338)   ECKCAQYWP--DQGCWTYGNVRVSVEDVTVLVDYTVRKFCIQQVGD-------VTNRKPQRLITQFHFTSWPDFGVPFTPIGMLKFLKKV
hPTPε-D1   (222)   EEKCHQYWP--DQGCWTYGNIRVCVEDCVVLVDYTIRKFCIQPQL--------PDGCKAPRLVSQLHFTSWPDFGVPFTPIGMLKFLKKV
hCD45-D1   (757)   RNKCAEYWPSMEEGTRAFGDVVVKINQHKRCPDYIIQKLNIVN----------KKEKATGREVTHIQFTSWPDHGVPEDPHLLLKLRRRV
hLAR-D1   (1447)   RVKCDQYWP--ARGTETCGLIQVTLLDTVELATYTVRTFALH----------KSGSSEKRE1RQFQFMAWPDHGVPEYPTPILAFLRRV
hPTPγ-D1   (958)   RRKCDQYWP--TENSEEYGNIIVTLKSTKIHACYTVRRFSIRNTKVKKGQKGNPKGRQNERVVIQYHYTQWPDMGVPEYALPVLTFVRRS

mPTPα-D2   (631)   QEKCAQYWP--SDGLVSYGDITVELKKEEECESYTVRDLLVT----------NTRENKSRQIRQFHFHGWPEVGIPSDGKGMINIIAAV
hPTPε-D2   (514)   QDKCYQYWP--TEGSVTHGEITIEIKNDTLSEAISIRDFLVTLNQPQ------ARQEEQVRVVRQFHFHGWPEIGIPAEGKGMIDLIAAV
hCD45-D2  (1067)   QEICAQYWG--EGKQTYGDIEVDLKDTDKSST-YTLRVFELR----------HSKRKDSRTVYQYQYTNWSVEQLPAEPKELISMIQVV
hLAR-D2   (1736)   REKCHQYWP--AERSARYQYFVVDPMAEYNMPQYILREFKVT----------DARDGQSRTIRQFQFTDWPEQGVPKTGEGFIDFIGQV
hPTPγ-D2  (1257)   AEDEFVYWP--SREESMNCEAFTVTLISKDRLCLSNEEQIIIHDFILE-----ATQDDYVLEVRHFQCPKWPNPDAPISSTFELINVIKE

Conserved-D1       --KC--YWP---------G---V----------Y-------------------------R---------WPD-GVP------L------
Conserved-D2       ------YW-------------------------------------------------------------W-----P--------------

                                      *     *
mPTPα-D1   (419)   KACNPQ---------YAGAIVVHCSAGVGRTGTFVVIDAMLDMMH-SERKVDVYGFVSRIRAQRCQMVQTDMQYVFIYQALLE
hPTPε-D1   (302)   KTLNPV---------HAGPIVVHCSAGVGRTGTFIVIDAMMAMMH-AEQKVDVFEFVSRIRNQRPQMVQTDMQYTFIYQALLE
hCD45-D1   (847)   NAFSNF---------FSGPIVVHCSAGVGRTGTYIGIDAMLEGLE-AENKVDVYGYVVKLRRQRCLMVQVEAQYILIHQALVE
hLAR-D1   (1524)   KACNPL---------DAGPMVVHCSAGVGRTGCFIVIDAMLERMK-HEKTVDIYGHVTCMRSQRNYMVQTEDQYVFIHEALLE
hPTPγ-D1  (1046)   SAARMP---------ETGPVLVHCSAGVGRTGTYIVIDSMLQQIK-DKSTVNVLGFLKHIRTQRNYLVQTEEQYIFIHDALLE

mPTPα-D2   (708)   QKQQQQ--------SGNHPITVHCSAGAGRTGTFCALSTVLERVKWAEGILDVFQTVKSLRLQRPHMVQTLEQYEFCYKVVQE
hPTPε-D2   (596)   QKQQQQ--------TGNHPITVHCSAGAGRTGTFIALSNILERVK-AEGLLDVFQAVKSLRLQRPHMVQTLEQYEFCYKVVQD
hCD45-D2  (1143)   KQKLPQKNSSEGNKHHKSTPLIHCRDGSQQTGIFCALLNLLESAE-TEEVVDIFQVVKALRKARLGMVSTFEQYQFLYDVIAS
hLAR-D2   (1813)   HKTKEQ--------FGQDGPITVHCSAGVGRTGVFITLSIVLERMR-YEGVVDMFQTVKTLRTQRPAMVQTEDQYQLCYRAALE
hPTPγ-D2  (1340)   EALTRD-----------GPTIVHDEYGAVSAGMLCALTTLSQQLE-NENAVDVFQVAKMINLMRPGVFTDIEQYQFIYKARLS

Conserved-D1       -----------------G---VHCSAGVGRTG----ID-M----------V---------R-QR---VQ---QY--I--AL-E
Conserved-D2       ----------------------H---G----G----L----------E---D-FQ--K-----R--------QY---Y-----
```

FIG. 2. **Sequence alignment of the PTPase domains of mouse PTPα (25), human PTPε (7), human CD45 (36), human LAR (37), and human PTPγ (38).** The invariant Cys and Arg residues in the PTPase signature motif, and the invariant Asp residue in the WPD motif are highlighted by an *asterisk* (*).

similar site-directed mutagenesis experiments with the invariant Asp residue have been performed with intracellular PTPases (4, 47), such experiments have not been done with receptor-like PTPases. Both bPTPα-D1/D401A and bPTPα-D2/E690D were expressed and purified similarly to near homogeneity as described for the wild-type D1 and D2. Using

TABLE III
Inhibition by phosphate, arsenate, vanadate, and p-nitrophenol
All measurements were made at pH 6 and 30 °C.

Inhibitor/enzyme	Inhibition constant (K_i)	Inhibition pattern
	mM	
Phosphate		
bPTPα	130 ± 16	Competitive
bPTPα-D1	120 ± 16	Competitive
bPTPα-D2	74 ± 5	Competitive
bPTPα-D2/E690D	37 ± 4	Competitive
Arsenate		
bPTPα	0.32 ± 0.02	Competitive
bPTPα-D1	0.25 ± 0.01	Competitive
bPTPα-D2	8.1 ± 0.3	Competitive
bPTPα-D2/E690D	8.3 ± 0.2	Competitive
Vanadate		
bPTPα	0.0049 ± 0.0003	Competitive
bPTPα-D1	0.0055 ± 0.0007	Competitive
bPTPα-D2	1.9 ± 0.4	Competitive
bPTPα-D2/E690D	1.0 ± 0.1	Competitive
p-Nitrophenol		
bPTPα	61 ± 14	Noncompetitive
bPTPα-D1	55 ± 12	Noncompetitive
bPTPα-D2	43 ± 15	Noncompetitive

*p*NPP as a substrate, the k_{cat} for bPTPα-D1/D401A is 900-fold slower than that of wild-type bPTPα-D1, while the K_m for bPTPα-D1/D401A is identical to that of bPTPα-D1 (Table I). These results are similar to those observed with cytoplasmic PTPases and suggest that Asp-401 is indeed important for the activity of D1 and that a common catalytic strategy is shared by both the receptor-like and soluble PTPases.

Asp substitution for Glu at 690 in bPTPα-D2 has modest effects on the kinetic parameters using *p*NPP as a substrate (Table I). A 4-fold increase in k_{cat} and nearly identical K_m were observed for bPTPα-D2/E690D when compared with the wild-type D2. In fact, bPTPα-D2/E690D has a k_{cat} value that is only 2-fold lower than that of bPTPα-D1 using *p*NPP as a substrate. Similar results were obtained with the Tyr(P)-containing peptides (Table II), namely D2/E690D displays 3–4-fold higher k_{cat} value and identical K_m value in comparison with the native D2 domain. However, the k_{cat} and k_{cat}/K_m values of bPTPα-D2/E690D toward Tyr(P)-containing peptides are still 3 and 4 orders of magnitude lower when compared with bPTPα-D1 (Table II). These results suggest that substitution of Glu-690 for an Asp in D2 may not be the main cause that D2 is a much less efficient phosphatase than D1 toward phosphopeptide substrates.

Inhibition by Inorganic Phosphate, Arsenate, Vanadate, and p-Nitrophenol—Inhibition constants were determined for inorganic phosphate, arsenate, vanadate, and *p*-nitrophenol at pH 6.0 (Table III). In general, effects of inhibitors to bPTPα-D1-catalyzed reaction are similar to that catalyzed by the double domain construct bPTPα. Substitution of Glu-690 by an Asp does not enhance significantly the affinity of bPTPα-D2 toward the oxyanions. Oxyanions were competitive inhibitors with respect to *p*NPP, whereas *p*-nitrophenol was noncompetitive. The pattern of product (phosphate and *p*-nitrophenol) inhibition suggests that D1 and D2 utilize a similar kinetic scheme (Scheme 1), particularly in terms of the order of addition of substrates and release of products (33). Inorganic phosphate usually shows K_i values around 1–5 mM against PTPases (33, 42, 48). Compared with other PTPases, bPTPα-D1 binds phosphate with an unusually weak affinity (K_i = 120 mM) which is even 2-fold lower than bPTPα-D2. Arsenate binds to bPTPα-D1 and bPTPα-D2 more tightly than phosphate, however, the increase in affinity is seen greater with bPTPα-D1 than bPTPα-D2. Thus, arsenate inhibits the bPTPα-D1-catalyzed reaction (K_i = 0.25 mM) 30-fold more potently than the bPTPα-D2-catalyzed reaction.

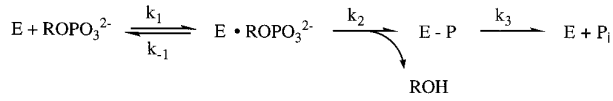

SCHEME 1. This scheme depicts a minimal kinetic mechanism for the PTPase-catalyzed reaction, which is composed of substrate binding, followed by two chemical steps, phosphorylation (k_2) and dephosphorylation (k_3) of the enzyme; where E is the enzyme, $ROPO_3^{2-}$ the substrate, $E{\cdot}ROPO_3^{2-}$ the enzyme-substrate Michaelis complex, E-P the phosphoenzyme intermediate, *ROH* the phenol or dephosphorylated peptide, and P_i inorganic phosphate.

Vanadate is by far the most potent small molecule inhibitor for PTPases. Because vanadate can adopt five-coordinate structures readily, it was expected that a covalent bond can be formed between the active site thiol and the vanadium atom. The structure of *Yersinia* PTPase complexed with vanadate revealed continuous electron density between the bound anion and the active site Cys-403, consistent with a covalent bond (49). Indeed, vanadate in the active site adopts a slightly distorted trigonal bipyramidal geometry that resembles the transition state for the hydrolysis of the thiophosphate enzyme intermediate in the PTPase-catalyzed reaction (6, 50). Previous studies with vanadate have often included EDTA in the assay buffers. Since EDTA forms a very stable 1:1 complex with vanadate even at micromolar concentrations of both EDTA and vanadate (51), the presence of EDTA in the assay solution will reduce the free vanadate concentration. Here we performed all of our inhibition experiments with vanadate in the absence of EDTA. Vanadate shows an apparent K_i of 5.5 μM toward bPTPα-D1 whereas the K_i for bPTPα-D2 is 1.9 mM. Thus, bPTPα-D1 binds vanadate 350-fold tighter than bPTPα-D2. Furthermore, bPTPα-D1 binds vanadate (a crude transition state analog) 22,000-fold more tightly than phosphate (a crude substrate analog), while bPTPα-D2 binds vanadate only 40-fold more tightly than phosphate. Since one of the major means an enzyme utilizes to catalyze a reaction is via transition state stabilization, it is understandable that bPTPα-D1 is a better PTPase than bPTPα-D2. Because vanadate can take on different forms in solution, and because the enzyme-bound vanadate has a different structure from the tetrahedral vanadate in solution, it is very likely that the kinetically determined K_i may underestimate how good a transition state analog the PTPase-bound vanadate really is (52).

pH Dependence—The pH dependence of the steady-state kinetic parameters for the various forms of PTPα were studied in detail using *p*NPP as a substrate. Within the pH range investigated, K_m values only exhibited moderate variations from those reported in Table I. The pH-k_{cat} profile is shown in Fig. 3. The line that is drawn through the experimental data is based on the nonlinear least-squares fit of the data to Equation 2. pK_1^{app}, pK_2^{app}, and the pH-independent maximum turnover number k_{cat}^{lim} are listed in Table IV. It appears that bPTPα-D1 displays a similar pH rate profile to that of bPTPα, except k_{cat}^{lim} for bPTPα is twice that of bPTPα-D1. Although substitution of an Asp in place of Glu-690 in bPTPα-D2 increase the k_{cat}^{lim} by 4-fold, it does not alter the pH rate profile. It is also clear that bPTPα-D1 and bPTPα-D2 display different pH rate profile: the pH optimum for bPTPα-D1-catalyzed hydrolysis of *p*NPP is 0.5 pH unit lower than that of bPTPα-D2.

Leaving Group Dependence—We have shown above that when compared with bPTPα-D1, the k_{cat} and k_{cat}/K_m values of bPTPα-D2 toward *p*NPP are reduced by 10- and 50-fold, respectively (Table I). On the other hand, when Tyr(P)-containing

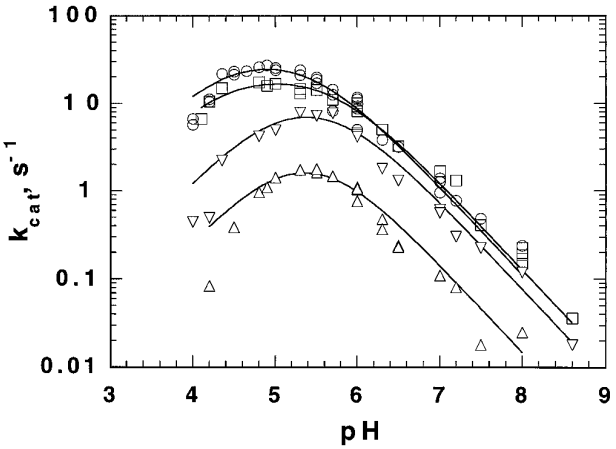

FIG. 3. **pH k_{cat} profile for the various forms of PTPα-catalyzed hydrolysis of *p*NPP.** ○, bPTPα; □, bPTPα-D1; △, bPTPα-D2; and ▽, bPTPα-D2/E690D. The *line* that is drawn through the experimental data is based on the nonlinear least-squares fit of the data to Equation 2.

TABLE IV
Kinetic parameters for PTPα-catalyzed hydrolysis of pNPP at 30 °C

PTPase	pK_1^{app}	pK_2^{app}	k_{cat}^{lim}
			s^{-1}
bPTPα	4.3 ± 0.2	5.5 ± 0.1	37 ± 1
bPTPα-D1	4.3 ± 0.1	5.7 ± 0.2	18 ± 0.4
bPTPα-D2	5.0 ± 0.1	5.7 ± 0.1	2.9 ± 0.2
bPTPα-D1/E690D	5.0 ± 0.1	5.8 ± 0.1	12 ± 1

peptides are used as substrates, up to 3 and 4 orders of magnitude reduction are observed with k_{cat} and k_{cat}/K_m, respectively (Table II). One possible explanation for this differential effects may be that Glu-690 in bPTPα-D2 is a weaker general acid than an Asp in bPTPα-D1, so that substrates with Tyr (pK_a = 10.07) as a leaving group becomes more difficult to expel because the negative charge developed on the phenolate oxygen in the transition state (47) cannot be efficiently stabilized by Glu-690. Leaving groups in substrates such as *p*NPP (pK_a = 7.14) are much easier to expel since there is much less demand for general acid catalysis.

To test this hypothesis, we investigated the leaving group dependence of the PTPase-catalyzed hydrolysis of aryl phosphates. Since Tyr(P)-containing peptides are more complex and different from *p*NPP in terms of structure, we chose several low molecular weight aryl phosphates to minimize the influence on the reaction by steric effects. As shown in Fig. 4, both bPTPα and bPTPα-D1 exhibit no leaving group dependence and show very similar k_{cat} values for hydrolysis of aryl phosphates that differ markedly in their leaving group pK_a (for example, 7.14 for *p*-nitrophenol and 10.26 for 4-methylphenol). Interestingly, bPTPα-D2 and bPTPα-D2/E690D display only moderate leaving group dependences, with β_{lg} values of −0.092 ± 0.041 and −0.11 ± 0.051, respectively. Thus although bPTPα-D2/E690D is four times more active than bPTPα-D2, it does not alter the leaving group sensitivity. From these observations, it appears that the 3–4 orders of magnitude decrease in reactivity toward Tyr(P)-containing peptides by bPTPα-D2 and bPTPα-D2/E690D is not due to the intrinsic lower stability of the Tyr leaving group. This is because, in comparison with *p*NPP, one would only predict a 2-fold decrease in rate for phosphotyrosine based on the leaving group dependences of bPTPα-D2 and bPTPα-D2/E690D catalyzed aryl phosphate hydrolysis reaction.

Peptide Substrate Amino Acid Sequence Specificity—Substrate specificity in terms of peptide size and amino acid sequence preference were investigated using Tyr(P)-containing peptides. The PTPase-catalyzed dephosphorylation reaction was continuously monitored spectrofluorimetrically (excitation at 280 nm and emission at 305 nm) at pH 6.0 and 30 °C. This assay takes advantage of the increase in fluorescence at 305 nm when the phosphate is hydrolyzed from Tyr(P) (30). At substrate concentrations $\ll K_m$, the Michaelis-Menten equation (Equation 1) reduces to Equation 3, and the reaction is first order with respect to [S]. With automatic data collection and nonlinear least square fit analysis, the first-order rate constant can be determined with a precision of less than 4%. The observed apparent first-order rate constant is equal to $(k_{cat}/K_m)[E]$, from which the substrate specificity constant k_{cat}/K_m value can be calculated by dividing the apparent first-order rate constant with the enzyme concentration. Additional advantages of this assay include that very small amount of peptide substrate is used per reaction and that accurate substrate concentration determination is not necessary. In general, substrate concentrations were at least 15-fold lower than the K_m values (Table II) and ranged from 2 to 10 μM. To ensure first-order kinetics, reactions were conducted at several substrate concentrations. Since the reaction is first order in nature, the same rate constant is obtained regardless the substrate concentration used. Because the k_{cat}/K_m values for bPTPα-D2 and bPTPα-D2/E690D are 5 orders of magnitude slower than those of bPTPα, they cannot be determined by the fluorescence assay.

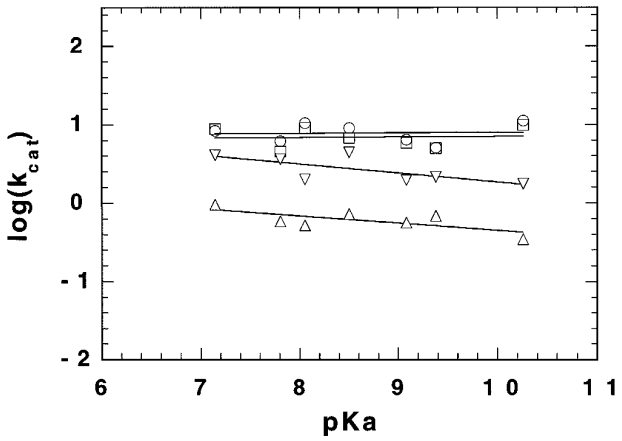

FIG. 4. **Leaving group dependence of the various forms of PTPα-catalyzed phosphate monoester hydrolysis.** Compounds that are included in the plots are *p*NPP, 4-methyl umbelliferyl phosphate, β-naphthyl phosphate, 4-acetylphenyl phosphate, 4-ethoxycarbonylphenyl phosphate, 3-chlorophenyl phosphate, and 4-methylphenyl phosphate. ○, bPTPα, □, bPTPα-D1; △, bPTPα-D2; and ▽, bPTPα-D2/E690D. The *lines* that are drawn through the experimental data are generated by a linear regression method.

The peptide substrate amino acid sequence specificity was probed with Tyr(P)-containing peptides corresponding to Tyr autophosphorylation sites in platelet-derived growth factor receptor, EGF receptor, Neu oncogene, Src kinase, or RPTPα (Table V). The substrate specificity constants (k_{cat}/K_m values) determined by the fluorescence assay are very similar to those calculated from the ratio of k_{cat} and K_m, which are determined by the initial rate method (Table II). In agreement with results described above, bPTPα and bPTPα-D1 display similar substrate specificity toward peptide substrates, but the k_{cat}/K_m values for bPTPα are slightly higher that those of bPTPα-D1, which is likely due to the slightly higher k_{cat} for bPTPα. In general, bPTPα and bPTPα-D1 only exhibit a moderate selectivity toward the various peptides. Only a 8-fold difference in k_{cat}/K_m was observed among the peptides. Although the enzyme does appear to prefer peptides with two acidic residues

TABLE V
Phosphopeptide substrate sequence specificity for bPTPα and bPTPα-D1

Peptides	bPTPα (k_{cat}/K_m)	bPTPα-D1 (k_{cat}/K_m)
	M^{-1} s^{-1}	
DADEpYLIPQQG (EGFR$^{988–998}$)	227,000 ± 3,000	163,000 ± 2,000
TAENAEpYLRV (EGFR$^{1167–1176}$)	66,700 ± 1,200	34,300 ± 400
LPVPEpYTNASV (EGFR$^{1063–1073}$)	89,500 ± 800	43,300 ± 100
ENPEpYLGLNVPV (Neu$^{572–583}$)	51,500 ± 500	23,800 ± 700
DAEEpYLVPQQG (Neu$^{347–357}$)	276,000 ± 8,000	182,000 ± 4,000
DTSSVLpYTAVQ (PDGFR$^{1003–1013}$)	180,000 ± 2,000	155,000 ± 600
EGDNDpYIIPL (PDGFR$^{1016–1025}$)	44,800 ± 200	30,100 ± 200
TEPQpYQPGE (p60^{src}523–531)	84,800 ± 1,400	41,500 ± 1,200
Ac-DAFSDpYANFK (PTPα$^{784–793}$)	34,700 ± 300	24,200 ± 800

TABLE VI
Minimum length of peptide substrate for bPTPα and bPTPα-D1

Peptides	bPTPα (k_{cat}/K_m)	bPTPα-D1 (k_{cat}/K_m)
	M^{-1} s^{-1}	
pY	208 ± 30[a]	154 ± 18[a]
Ac-Tyr(P)-NH_2	15,800 ± 100	12,700 ± 290
EpYL	980 ± 10	690 ± 15
EpYLI	1,900 ± 40	1,600 ± 37
DEpYL	1,490 ± 19	1,670 ± 13
Ac-EpYL	25,400 ± 190	22,400 ± 240
DEpYLI	84,200 ± 1,200	82,600 ± 840
ADEpYLI	148,000 ± 700	136,000 ± 2,100
ADEpYLIP	185,000 ± 7,000	168,000 ± 6,000
Ac-ADEpYLI	112,000 ± 2,000	101,000 ± 400
Ac-DADEpYL	22,700 ± 100	9,540 ± 140
Ac-DADEpYLI	47,000 ± 300	21,200 ± 100
pYLIPQQG	ND[b]	ND[b]
DADEpY-NH_2	133,000 ± 2,100	118,000 ± 1,300
DADEpYL-NH_2	32,600 ± 150	34,300 ± 230
DADEpYLIPQQG (EGFR$^{988–998}$)	227,000 ± 3,000	163,000 ± 2,000

[a] The k_{cat}/K_m value for phosphotyrosine cannot be determined by the fluorescence assay. The k_{cat} and K_m values were determined by following the production of tyrosine (using an absorption coefficient of 2400 at 293nm) at several phosphotyrosine concentrations (29).
[b] ND, the k_{cat}/K_m value cannot be determined by the fluorescence assay.

immediately NH_2-terminal to Tyr(P) (DADEpYLIPQQG and DAEEpYLVPQQG), there is also exception to this (DTSSVLpYTAVQ).

The Minimum Length of a Peptide Substrate—To determine the minimum length of a peptide substrate for bPTPα and bPTPα-D1, we selected a series of various sized phosphopeptides modeled after the autophosphorylation site in EGF receptor (EGFR) at Tyr-992 (Table VI). For the sake of discussion, we will focus the results on bPTPα, since identical conclusions can be reached from results on bPTPα-D1. Phosphotyrosine (Tyr(P)) by itself is not a good substrate. In fact, its k_{cat}/K_m value cannot be determined by the fluorescence assay because of the slow rate. We therefore determined its k_{cat} and K_m by the initial rate method using a molar absorption coefficient of 2,400 for tyrosine (29). The calculated k_{cat}/K_m values for Tyr(P) are listed in Table VI. It seems that the low k_{cat}/K_m for Tyr(P) is primarily due to its high K_m: 22.1 mM for bPTPα (19.5 mM for bPTPα-D1). As shown in Table VI, the k_{cat}/K_m value for the parent peptide DADEpYLIPQQG (EGFR$^{988–998}$) is 1090-fold higher than Tyr(P). This indicates that structural elements surrounding Tyr(P) in the peptide contribute to specificity.

Strikingly, Ac-Tyr(P)-NH_2, which is obtained by acetylating the free amino group and amidating the free carboxyl group of Tyr(P), exhibit a k_{cat}/K_m that is 76-fold higher than Tyr(P). Interestingly, the tripeptide EpYL is only 4.7-fold better than Tyr(P). Since acetyl group is smaller than a Glu residue, the dramatic enhancement in substrate efficacy for Ac-Tyr(P)-NH_2 seems to mainly arise from the elimination of charges on the free amino and carboxyl groups, rather than the increase in size. The addition of an Ile to the COOH-terminal side of EpYL (generating EpYLI) results in only a 1.9-fold improvement, while addition of an Asp to NH_2-terminal side of EpYL (generating DEpYL) leads to a 1.5-fold increase in activity. Although the acetyl group is smaller than an Asp residue, the kinetic parameter for Ac-EpYL is 17-fold higher than that of DEpYL. This may again be due to the elimination of the positive charge on the NH_2-terminal amino group of EpYL.

The incorporation of an additional residue, Ile, to the COOH-terminal side of DEpYL produces a pentapeptide (DEpYLI) that is 56 times more efficient than DEpYL. Thus, the extension of DEpYL beyond the +1 position by one residue is more than enough to offset the undesirable charge effect on the NH_2-terminal side. Further extension at the NH_2-terminal of DEpYLI by an Ala (to give ADEpYLI) improves its efficacy by 1.8-fold. Attachment of a Pro residue to the COOH-terminal of peptide ADEpYLI does not produce significant increase in substrate specificity, whereas attachment of an acetyl group to the NH_2-terminal of peptide ADEpYLI actually reduces its efficiency slightly (by 1.3-fold). This suggests that the hexapeptide ADEpYLI may represent a minimal peptide substrate for bPTPα and bPTPα-D1. In fact, the k_{cat}/K_m value for ADEpYLI is within 1.5-fold of the parent peptide DADEpYLIPQQG. We are surprised by the observation that in the absence of additional residues beyond the +2 position in ADEpYLI, elongation at the NH_2-terminal side (*e.g.* Ac-DADEpYLI) interferes with bPTPα activity. However Ac-DADEpYLI is still about twice as efficient as Ac-DADEpYL, consistent with the importance of residues at the +2 position noted above.

We also investigated whether residues on the NH_2- or COOH-terminal side of Tyr(P) are more important in determining bPTPα substrate specificity. When all of the residues NH_2-terminal to the Tyr(P) of EGFR$^{988–998}$ are removed, the resulting peptide pYLIPQQG is such a poor substrate that its k_{cat}/K_m value cannot be determined by the fluorescence method. Due to the limited amount of material, we could not measure its k_{cat} and K_m by the initial rate method. Since the lowest k_{cat}/K_m value determined by the fluorescence assay is 690 M^{-1} s^{-1} (for the bPTPα-D1-catalyzed hydrolysis of EpYL), we assume it as an upper limit for pYLIPQQG. Thus, pYLIPQQG behaves kinetically similarly to phosphotyrosine. This could either indicate that positive charge on the amino group of Tyr(P) is deleterious or that residues COOH-terminal to Tyr(P) are not important for binding. Judging from the results described above, the former possibility is most likely. Further experiments are required to resolve this. Interestingly, when all of the residues COOH-terminal to the Tyr(P) are removed from EGFR$^{988–998}$ and the negative charge on the free carboxylate eliminated by amidation, the k_{cat}/K_m value of the pentapeptide DADEpY-NH_2 approaches that of the parent peptide. Surprisingly, the hexapeptide DADEpYL-NH_2, which is obtained by incorporating just one more Leu residue to the COOH-terminal side of Tyr(P) in DADEpYL-NH_2, shows a 4-fold decrease in substrate specificity in comparison with the pentapeptide. Thus, it appears that in the absence of charge and additional residues on the COOH-terminal side of Tyr(P), four residues NH_2-terminal to Tyr(P) can serve as an effective substrate. Collectively, from a systematic analysis of different fragments of EGFR$^{988–998}$ peptide, we conclude that efficient binding and

catalysis by bPTPα and bPTPα-D1 require minimally either six amino acids (including Tyr(P), three residues NH_2- and two residues COOH-terminal to Tyr(P)) or five amino acids (including Tyr(P)-NH_2 and four residues NH_2-terminal to Tyr(P)).

DISCUSSION

PTPα is a representative of the receptor-like PTPases that contains two PTPase domains. In this paper we try to address whether both of the PTPase domains in PTPα are active, and if both are active, what are the relative contributions for each domain to the double domain molecule. We have compared the kinetic properties of bPTPα, bPTPα-D1, and bPTPα-D2 using near homogeneous preparations of recombinant proteins. We demonstrate that bPTPα-D1 and bPTPα (containing two tandem PTPase domains) display similar steady-state kinetic parameters, pH and leaving group dependences, sensitivity to oxyanion and *p*-nitrophenol inhibitors, and substrate specificity. This suggests that the catalytic activity of PTPα is dominated by the D1 domain and that the D2 domain does not contribute significantly to the overall property of the double domain construct. This is likely due to the fact that the k_{cat} for D2 is much reduced and the K_m for D2 is much elevated when compared with those of D1, especially in cases of phosphopeptide substrates.

The three-dimensional structure of RPTPα-D1 (containing residues 202–503) has been determined (53). This particular D1 construct crystallized as a homodimer. It was found that a segment of the NH_2-terminal sequence (residues 208–242) of one monomer formed a helix-turn-helix structural wedge which tucked into the active site of the dyad-related monomer. This restrained the WPD loop of each monomer in the open (inactive) conformation and would block potential substrate binding. The D1 construct used in this study contains amino acids from 167 to 503 (Fig. 1). We find that under our assay conditions both bPTPα-D1 and bPTPα are active. Furthermore, at bPTPα-D1 concentration between 10 and 100 nM, the apparent first-order rate constant for the hydrolysis of Tyr(P)-containing peptides is strictly first-order with respect to the enzyme concentration with a zero *y* intercept when the rate constant is plotted against enzyme concentration (data not shown), consistent with bPTPα-D1 exists as an active monomer in solution.

We also demonstrate that the D2 domain of PTPα is a genuine PTPase in its own right. This is especially true when low molecular weight aryl phosphates are used as substrates. In fact, the k_{cat} value for D2 is only 10-fold lower than that of D1 while the K_m is 5-fold elevated with *p*NPP as a substrate. However, the D2-catalyzed reaction shows different pH and leaving group dependences from that of D1. It also possesses a much lower affinity to the transition state analog vanadate and greatly reduced k_{cat} and k_{cat}/K_m values for peptide substrates. In a previous study, the V_{max} and K_m values for the D2 domain of human PTPα-catalyzed hydrolysis of a Tyr(P)-containing peptide (RR-Src) were shown to be 200-fold lower and 47-fold higher, respectively, when compared with the D1 domain (23). These differences in k_{cat} and K_m between D1 and D2 fall within the range that we observed with peptide substrates. However, from the same study, the V_{max} value for the D2-catalyzed hydrolysis of *p*NPP was shown to be 1.6-fold higher than that of D1. We do not know what causes the discrepancy regarding the *p*NPP data, except to note that in the previous study, D1 domain included residues from 167 to 542 whereas D2 domain included residues from 487 to 774 (23), which are different from the constructs we made in this work (Fig. 1).

We hypothesized that the large differences in catalytic properties between D1 and D2 might be caused by structural variations between the active sites of the two PTPase domains. Amino acid sequence alignment of both D1 and D2 from a number of receptor-like PTPases reveals that the D2 domain of PTPα contains all the essential features found in the PTPase signature motifs of cytoplasmic PTPases and the D1 domains of receptor PTPases. In addition to the fact that D1 domains are more conserved and homologous to the catalytic domains of cytoplasmic PTPases than D2 domains, the most apparent difference is that the putative general acid (Asp residue) in the WPD motif observed in all D1 domains and all cytoplasmic PTPases has been changed to Glu-690 in bPTPα-D2. We illustrate that mutation of Asp-401 in the WPD motif of bPTPα-D1 to an Ala decreases the k_{cat} by 900-fold, confirming the importance of general acid/base in the D1 domain of receptor PTPases. Replacement of Asp with Glu or vice versa can have dramatic effects in enzymes that require a carboxylate group as a general acid/base (43–46). Interestingly, the restoration of the general acid/base to an Asp at position 690 in bPTPα-D2 only raises the activity by 4-fold. This is consistent with our previous mutational studies of the general acid Asp-128 in the low molecular weight PTPase: D128E retained 15% of the native catalytic activity (42). Furthermore, substitution of Glu-690 by an Asp in bPTPα-D2 does not alter its pH and leaving group dependences, its sensitivity to oxyanion inhibitors, and its substrate specificity. Collectively, these results indicate that the active site of PTPase is fairly flexible and can tolerate a 1 methylene unit lengthened side chain as long as the carboxylate functionality is preserved.

It is interestingly to note that the phosphatase activity of D2 toward aryl phosphates are comparable to that of D1, but its activity toward Tyr(P)-containing peptides/proteins is much reduced (this work and Refs. 23 and 24). Since the k_{cat} for bPTPα-D2 catalyzed hydrolysis of 4-methylphenyl phosphate (pK_a of 4-methylphenol = 10.26) is only 2–3-fold slower than that of *p*NPP (pK_a of *p*-nitrophenol = 7.14), the very low activity toward peptide substrates is unlikely due to the higher pK_a of tyrosine (10.07). This together with the fact that Glu-690 to Asp substitution did not restore D2's activity to D1 suggest structural features other than the general acid/base residue may be responsible for the low activity toward peptide substrates. A three-dimensional structure for the D2 domain may shed more light on this. On the other hand, the reduced activity toward peptide substrates may also suggest that bPTPα-D2 has a functional active site with a highly stringent substrate selectivity. Thus, the configuration of active site residues in D2 responsible for binding and/or catalysis may not be optimal for nonspecific peptide substrates that require extensive intermolecular interactions. The possibility that there exists physiological substrate(s) for the D2 domain of PTPα remains to be explored.

The k_{cat} values for the bPTPα and bPTPα-D1 catalyzed hydrolysis of aryl phosphates and Tyr(P)-containing peptides are similar. This is consistent with the rate-determining step being the hydrolysis of the phosphoenzyme intermediate (*E*-P in Scheme 1) (6). The rate-limiting step for the D2-catalyzed hydrolysis of low molecular weight aryl phosphates may be predominately determined by *E*-P hydrolysis as well, given the small β_{lg} value observed. The fact that k_{cat} values for phosphopeptides are 40–160-fold slower than small aryl phosphates such as *p*NPP in the D2-catalyzed reactions suggest that the rate-limiting step for peptide substrates may be changed to the formation of *E*-P. This is consistent with the notion that the D2 domain may recognize a global conformation and require a precise alignment between residues in the enzyme active site and the specific substrate. Nonspecific peptide substrates may not be capable of forming productive enzyme-substrate complexes for the forward reaction.

Detailed kinetic analysis of bPTPα and bPTPα-D1 catalyzed

Tyr(P)-containing peptides show moderate selectivity toward different substrates. Our data also indicate that positive charges from the free amino group at Tyr(P), −1, and −2 positions and the negative charge of the free carboxylate at Tyr(P) can be detrimental to PTPα catalysis. We have shown previously that in the sequence context of DADEpYLIPQQG ($EGFR^{988-998}$), the *Yersinia* PTPase, and the mammalian PTP1 require a minimum of six amino acid residues for most efficient binding and catalysis (54). These include Tyr(P), four amino acid residues NH_2-terminal, and one amino acid residue COOH-terminal to the Tyr(P) (DADEpYL-NH_2). Using the same series of peptides, we conclude that for optimal PTPα activity the minimal size of peptide substrates can either be ADEpYLI or DADEpY-NH_2. Thus, different PTPases may possess different active site specificity in terms of short peptide substrates. It appears that short optimal peptides can be accommodated in the active site of the D1 domain by more than one mode. Furthermore, the recognition between PTPα and short peptide substrates seems sensitive to structural modifications.

Further understanding of the specific functional roles of PTPases in cellular signaling requires detailed investigation of PTPase substrate specificity. Clearly, a more systematic and thorough approach, such as the use of degenerate peptide libraries containing randomized amino acid residues surrounding the phosphotyrosine, is needed for the search of consensus sequence motif for individual PTPases. Although consensus peptide motifs of many protein kinases have been elucidated (55), those of PTPases are essentially unknown. Specific consensus peptide motif for PTPases will lay the foundation for structure based rational PTPase inhibitor design. Since the identity of the physiological substrates for most PTPases is not known at present, such optimal substrate motifs may also be useful for the identification of physiological substrates for PTPases from available protein sequence data bases.

Finally, based on the kinetic data and the comparison of the amino acid sequence alignment of D1 and D2 from a number of receptor-like PTPases presented in this paper, we suggest that D2 domains of certain types of receptor-like PTPases (*e.g.* PTPα, PTPε, and LAR) should display significant intrinsic phosphatase activity whereas D2 domains of other PTPases may possess little (*e.g.* CD45) or no (*e.g.* PTPγ) phosphatase activity. The functional role of the second domain, *i.e.* whether it regulates the specificity and activity of the first domain and/or exhibits independent substrate selectivity, requires further investigations.

REFERENCES

1. Sun, H. & Tonks, N. K. (1994) *Trends Biochem. Sci.* **19,** 480–485
2. Hunter, T. (1995) *Cell* **80,** 225–236
3. Walton, K. & Dixon, J. E. (1993) *Annu. Rev. Biochem.* **62,** 101–120
4. Zhang, Z.-Y., Wang, Y. & Dixon, J. E. (1994) *Proc. Natl. Acad. Sci. U. S. A.* **91,** 1624–1627
5. Zhang, Z.-Y., Wang, Y., Wu, L., Fauman, E., Stuckey, J. A., Schubert, H. L., Saper, M. A. & Dixon, J. E. (1994) *Biochemistry* **33,** 15266–15270
6. Zhang, Z.-Y. (1997) *Curr. Top. Cell. Regul.* **35,** 21–68
7. Krueger, N. X., Streuli, M. & Saito, H. (1990) *EMBO J.* **9,** 3241–3252
8. Levy, J. B., Canoll, P. D., Silvennoinen, O., Barnea, G., Morse, B., Honegger, A. M., Huang, J.-T., Cannizzaro, L. A., Park, S.-H., Druck, T., Huebner, K., Sap, J., Ehrlich, M., Musacchio, J. M. & Schlessinger, J. (1993) *J. Biol. Chem.* **268,** 10573–10581
9. Tian, S.-S., Tsoulfas, P. & Zinn, K. (1991) *Cell* **67,** 675–685
10. Yang, X., Seow, K. T., Bahri, S. M., Oon, S. H. & Chia, W. (1991) *Cell* **67,** 661–673
11. Wang, Y. & Pallen, C. J. (1992) *J. Biol. Chem.* **267,** 16696–16702
12. Streuli, M., Krueger, N. X., Tsai, A. Y. & Saito, H. (1989) *Proc. Natl. Acad. Sci. U. S. A.* **86,** 8698–8702
13. Streuli, M., Krueger, N. X., Thai, T., Tang, M. & Saito, H. (1990) *EMBO J.* **9,** 2399–2407
14. Itoh, M., Streuli, M., Krueger, N. X. & Saito, H. (1992) *J. Biol. Chem.* **267,** 12356–12363
15. Cho, H., Ramer, S. E., Itoh, M., Kitas, E., Bannwarth, W., Burn, P., Saito, H. & Walsh, C. T. (1992) *Biochemistry* **31,** 133–138
16. den Hertog, J., Pals, C. E. G. M., Peppelenbosch, M. P., Tertoolen, L. G. J., de Laat, S. W. & Kruijer, W. (1993) *EMBO J.* **12,** 3789–3798
17. Desai, D. M., Sap, J., Silvennoinen, O., Schlessinger, J. & Weiss, A. (1994) *EMBO J.* **13,** 4002–4010
18. Pot, D. A., Woodford, T. A., Remboutsika, E., Haun, R. S. & Dixon, J. E. (1991) *J. Biol. Chem.* **266,** 19688–19696
19. Gebbink, M. F. B. G., Verheijen, M. H. G., Zondag, G. C. M., van Etten, I. & Moolenaar, W. H. (1993) *Biochemistry* **32,** 13512–13522
20. Tan, X., Stover, D. R. & Walsh, K. A. (1993) *J. Biol. Chem.* **268,** 6835–6838
21. Johnson, P., Ostergaard, H. L., Wasden, C. & Trowbridge, I. S. (1992) *J. Biol. Chem.* **267,** 8035–8041
22. Ng, D. H., Maiti, A. & Johnson, P. (1995) *Biochem. Biophys. Res. Commun.* **206,** 302–309
23. Wang, Y. & Pallen, C. J. (1991) *EMBO J.* **10,** 3231–3237
24. den Hertog, J., Tracy, S. & Hunter, T. (1994) *EMBO J.* **13,** 3020–3032
25. Sap, J., D'Eustachio, P., Givol, D. & Schlessinger, J. (1990) *Proc. Natl. Acad. Sci. U. S. A.* **87,** 6112–6116
26. den Hertog, J., Overvoorde, J. & de Laat, S. W. (1996) *Mech. Dev.* **58,** 89–101
27. Zheng, X. M., Wang, Y. & Pallen, C. J. (1992) *Nature* **359,** 336–339
28. Moller, N. P. H., Moller, K. B., Lammers, R., Kharitonenkov, A., Hoppe, E., Wiberg, F. C., Sures, I. & Ullrich, A. (1995) *J. Biol. Chem.* **270,** 23126–23131
29. Zhang, Z.-Y. & VanEtten, R. L. (1991) *J. Biol. Chem.* **266,** 1516–1525
30. Zhang, Z.-Y., Maclean, D., Thieme-Sefler, A. M., Roeske, R. & Dixon, J. E. (1993) *Anal. Biochem.* **211,** 7–15
31. Guan, K. L. & Dixon, J. E. (1991) *Anal. Biochem.* **192,** 262–267
32. Zhang, Z.-Y., Palfey, B. A., Wu, L. & Zhao, Y. (1995) *Biochemistry* **34,** 16389–16396
33. Zhang, Z.-Y. (1995) *J. Biol. Chem.* **270,** 11199–11204
34. Gordon, J. A. (1991) *Methods Enzymol.* **201,** 477–482
35. Chen, L., Montserat, J., Lawrence, D. S. & Zhang, Z.-Y. (1996) *Biochemistry* **35,** 9349–9354
36. Streuli, M., Hall, L. R., Saga, Y., Schlossman, S. F. & Saito, H. (1987) *J. Exp. Med.* **166,** 1548–1566
37. Streuli, M., Krueger, N. X., Hall, L. R., Schlossman, S. F. & Saito, H. (1988) *J. Exp. Med.* **168,** 1523–1530
38. Barnea, G., Silvennoinen, O., Shaanan, B., Honegger, A. M., Canoll, P. D., D'Eustachio, P., Morse, B., Levy, J. B., LaForgia, S., Huebner, K., Musacchio, J., Sap, J. & Schlessinger, J. (1993) *Mol. Cell. Biol.* **13,** 1497–1506
39. Guan, K. & Dixon, J. E. (1991) *J. Biol. Chem.* **266,** 17026–17030
40. Wo, Y.-Y. P., Zhou, M.-M., Stevis, P., Davis, J. P., Zhang, Z.-Y. & Van Etten, R. L. (1992) *Biochemistry* **31,** 1712–1721
41. Cho, H., Krishnaraj, R., Kitas, E., Bannwarth, W., Walsh, C. T. & Anderson, K. S. (1992) *J. Am. Chem. Soc.* **114,** 7296–7298
42. Wu, L. & Zhang, Z.-Y. (1996) *Biochemistry* **35,** 5426–5434
43. Straus, D., Raines, R., Kawashima, E., Knowles, J. R. & Gilbert, W. (1985) *Proc. Natl. Acad. Sci. U. S. A.* **82,** 2272–2276
44. Hibler, D. W., Stolowich, N. J., Reynolds, M. A. & Gerlt, J. A. (1987) *Biochemistry* **26,** 6278–6286
45. Zawrotny, M. E. & Pollack, R. M. (1994) *Biochemistry* **33,** 13896–13902
46. Leung, Y.-C., Robinson, C. V., Aplin, R. T. & Waley, S. G. (1994) *Biochem. J.* **299,** 671–678
47. Hengge, A. C., Sowa, G, Wu, L. & Zhang, Z.-Y. (1995) *Biochemistry* **34,** 13982–13987
48. Zhang, Z.-Y., Malachowski, W. P., Van Etten, R. L. & Dixon, J. E. (1994) *J. Biol. Chem.* **269,** 8140–8145
49. Denu, J. M., Lohse, D. L., Vijayalakshmi, J., Saper, M. A. & Dixon, J. E. (1996) *Proc. Natl. Acad. Sci. U. S. A.* **93,** 2493–2498
50. Zhao, Y. & Zhang, Z.-Y. (1996) *Biochemistry* **35,** 11797–11804
51. Crans, D. C. (1994) *Comments Inorg. Chem.* **16,** 1–33
52. Gresser, M. J. & Tracy, A. S. (1990) in *Vanadium in Biological Systems: Physiology and Biology* (Chasteen, N. D., ed) pp. 63–79, Kluwer Academic Publishers, The Netherlands
53. Bilwes, A. M., den Hertog, J., Hunter, T. & Noel, J. P. (1996) *Nature* **382,** 555–559
54. Zhang, Z.-Y., Maclean, D., McNamara, D. J., Sawyer, T. K. & Dixon, J. E. (1994) *Biochemistry* **33,** 2285–2290
55. Kennelly, P. J. & Krebs, E. G. (1991) *J. Biol. Chem.* **266,** 15555–15558